Investigation of the Shear-Sliding Behavior of Masonry Through Shove Test: Experimental and Numerical Studies

Francesca Ferretti[1], Samira Jafari[2(✉)], Rita Esposito[2], Jan G. Rots[2], and Claudio Mazzotti[1]

[1] Department of Civil, Chemical, Environmental and Materials Engineering, University of Bologna, Bologna, Italy
{francesca.ferretti10, claudio.mazzotti}@unibo.it
[2] Department of Structural Engineering, Delft University of Technology, Delft, The Netherlands
{s.jafari, r.esposito, j.g.rots}@tudelft.nl

Abstract. To assess the shear properties of masonry for existing buildings, the shove test method proposed by ASTM C1531 can be carried out, in which the load required to slide a single brick with respect to the surrounding masonry is measured. To control the vertical stress-state on the tested brick, two flat-jacks can be inserted in mortar bed joints in close proximity of it, thus prescribing a predefined level of compression. Although this test seems straightforward, uncertainties have not been resolved yet regarding the actual vertical compressive stress present on the tested brick and the effect of dilatancy. To gain a better insight into the shear-sliding behavior of masonry during the shove test, both experimental tests and numerical simulations were considered in the current research. To analyze these aspects and to precisely define a testing protocol, the experimental tests were performed in a controlled laboratory environment on a single wythe calcium silicate brick masonry wall. In parallel, numerical analyses were carried out using a simplified micro-modeling strategy, in which every brick was modelled, and the mortar joints were considered as zero-thickness interfaces. A composite interface model was used, including a tension cut-off, a Coulomb friction domain and a compressive cap. For the analyzed case study, the numerical results allowed to gain a better understanding of the aspects influencing the shear-sliding behavior of masonry during the shove test.

Keywords: Unreinforced masonry · Calcium silicate bricks · Testing protocol
Laboratory environment · Simplified micro-modeling

1 Introduction

The shear-sliding failure of a masonry panel is strongly related to the local failure at unit-joints interface. Often a Coulomb friction criterion, based on the local properties in terms of initial shear strength and friction coefficient, is adopted to describe the local failure. To determine these properties in-situ the shove test, standardized in ASTM C1531-16 [1], is used. It consists in inducing the sliding of a single brick with respect

to the surrounding masonry. Even if the shear-sliding resistance of a single unit is not, strictly speaking, the same as the shear resistance of a masonry wall, the shove test still yields the most accurate and direct approximation of the in-situ shear strength [2]. According to the ASTM standard [1], the vertical compression can be directly applied by means of two flat-jacks, positioned above and below the tested brick. In this way, the compressive stress level is controlled for the entire duration of the test and, if single and double flat-jack tests are previously executed, the state of stress and the deformability properties of masonry can be evaluated as well.

Although the shove test seems straightforward, two main issues should be highlighted regarding the elaboration of the results. Firstly, there are uncertainties about the effective level of the normal compressive stress acting on the sliding brick. This can be associated to several factors, such as the removal of the two bricks placed adjacent to the tested brick, which cause a great disturbance of the wall integrity, and the dilatant behavior of mortar joints. Consequently, the actual stress distribution could significantly differ from the assumed uniform one imposed by the flat-jacks. Secondly, it is not well specified in the Standard [1] that the shear strength obtained from the first load step is associated with an initial Coulomb friction failure criterion (characterized by initial cohesion c_0 and initial friction angle ϕ_0). The values of the shear strength established from the subsequent steps, where the compression load is increased, describe instead a pure frictional behavior of the bed joints and have to be associated to a residual Coulomb friction domain (characterized by a residual friction angle ϕ_{res}). In this paper, the experimental and numerical studies are integrated aiming to address the two aforementioned issues.

2   Materials and Methods

In an experimental campaign conducted at Delft University of Technology, shove tests were performed on a replicated single-wythe calcium silicate brick masonry wall to determine the local properties of unit-joints interfaces. In this paper, one test will be presented in detail. It was performed according to the setup presented in Fig. 1. For the construction of the wall, calcium silicate bricks (dimensions: $214 \times 102 \times 72$ mm^3) and cementitious mortar (joint thickness: 10 mm) were used. To simulate the in-situ state of stress, an overburden load was applied at the top of the wall, by pre-stressing four steel rods linked to a transverse beam. The shove test was performed in the lower portion of the wall, applying an overburden load such as to obtain a nominal vertical compressive stress equal to 0.25 MPa at the height where the flat-jack was inserted.

In order to evaluate the contribution of the flat-jack pressure to the effective compressive stress on the sliding brick, the method proposed by Rossi et al. [3] is adopted. Accordingly, the double flat-jack test is performed before the shove test (*standard configuration*), as prescribed by ASTM C1197-14a, and in the *shove test configuration*, where the two bricks adjacent to the sliding brick are removed. Consequently, a flat-jack to brick correction factor can be assessed as the ratio between the Young's modulus E and the fictitious Young's modulus E^*, calculated from tests in the *standard* and in the *shove test configuration*, respectively. Multiplying the nominal flat-jack pressure by the flat-jack to brick correction factor (E/E^*), an effective
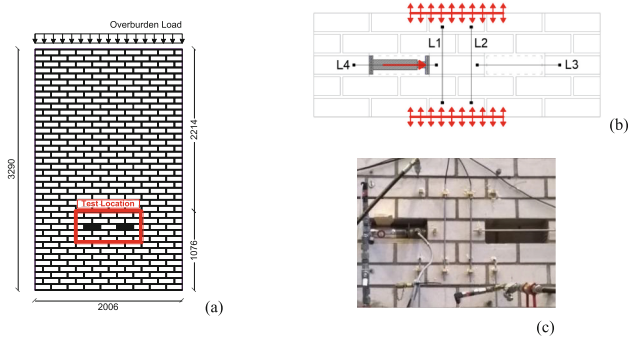
Fig. 1. Shove test setup: (a) calcium silicate brick wall; (b) test setup; (c) tested masonry portion

pre-compression value σ_j can be obtained, which is more representative of the real vertical stress state on the tested brick.

The testing procedure is as follow: (i) perform the double flat-jack test to estimate the Young's modulus of masonry in the *standard configuration E*; (ii) remove the two bricks adjacent to the tested brick; (iii) perform the double flat-jack test to evaluate the fictitious Young's modulus *E** in the *shove test configuration* [3]; (iv) apply a vertical pre-compression stress by loading the flat-jacks; (v) increase the pressure in the horizontal jack to obtain the sliding failure of the tested unit. For the presented case, a very low value of pressure in the two flat-jacks was set ($\sigma_1 = 0.065$ MPa) and kept constant. After the attainment of the first sliding, steps *iv* and *v* were repeated several times with increased levels of vertical pre-compression stress in the flat-jacks.

During the shove test, horizontal and vertical displacements were measured by means of LVDTs (measuring range of 10 mm with an accuracy of ±0.001 of LVDT's length): two horizontal LVDTs were positioned on both sides of the sliding brick to measure its relative displacement with respect to the surrounding masonry, and two vertical LVDTs were positioned across the sliding brick, to monitor the displacements orthogonal to the mortar joint (dilatancy) during the sliding failure. Moreover, LVDTs were placed outside of the tested masonry portion to check undesired failure modes, e.g. failure of the contrast portion behind the horizontal jack.

3   Experimental Results

The experimental results are described in this section. The Young's moduli obtained from the double flat-jack tests performed both in the *standard configuration* and in the *shove test configuration* are listed in Table 1. Moreover, the flat-jack to brick correction factor, calculated accordingly to Sect. 2, is also reported. Note that the Young's moduli were calculated as the most linear part of the stress-strain curve (i.e. chord moduli), while only the displacements of the vertical LVDTs positioned across the sliding brick (L1 and L2 in Fig. 1*b*) were taken into consideration.

The variation of the shear and of the vertical pre-compression stresses during the shove test is plotted in Fig. 2*a*. The testing phases can be classified as follows:

Table 1. Summary of the results of the double flat-jack tests.

Young's modulus in the *standard configuration* (E) MPa	Fictitious Young's modulus in the *shove test configuration* (E^*) MPa	Jack to brick correction factor (E/E^*)
7945	6750	1.18

(*i*) the initial phase, in which the shear load can be associated with both cohesion and friction and (*ii*) the residual phase, where failure at the brick-mortar interface has already occurred, thus the shear load can be associated only with a frictional behavior.
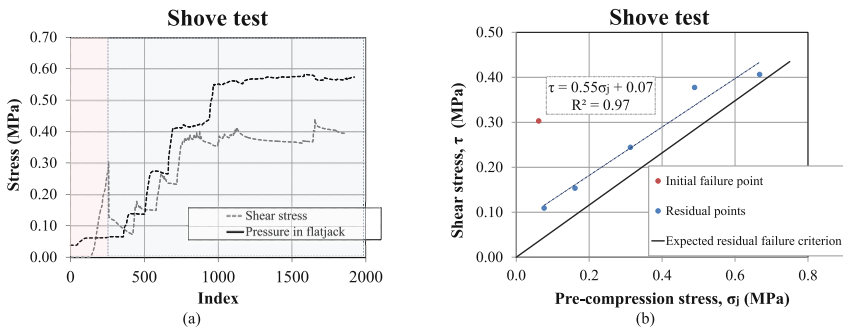
Fig. 2. Shove test: (a) variation of the shear stress and pre-compression stress within the test; (b) shear stress *vs* pre-compression stress.

The initial and the residual phase's states of stress (σ_j, τ) are plotted in Fig. 2*b*. It should be pointed out that the modified values of the pre-compression stress (σ_j), accounting for the modification of the flat-jack pressure due to the diffusion phenomenon occurring around the sliding brick, are reported. Using a linear interpolation of the failure points obtained in the residual phase at different vertical pressures, the residual properties of the masonry can be evaluated by considering the Coulomb friction failure domain. The residual cohesive shear strength (in correspondence of $\sigma_j = 0$) and the residual coefficient of friction are found as 0.07 MPa and 0.55, respectively. Since these parameters are associated with the residual properties, a zero value for the residual cohesive shear strength is expected. The inconsistency observed between expected residual cohesive shear strength and the one obtained from the shove test can be attributed to the fact that the nominal vertical compressive stress on the tested brick was not adjusted according to the overburden pressure variation in the shove test configuration. Due to the removal of bricks, the overburden pressure (originally uniform) partially deviates inward on the tested brick, influencing its state of stress. To obtain a null residual cohesive shear strength, the regression line evaluated for the residual points should be horizontally translated, adding to the σ_j values the overburden contribution to the vertical compressive stress of the tested unit [3]. To this purpose, an overburden correction factor (to be multiplied by the nominal overburden

to obtain the overburden contribution) will be evaluated using numerical model, as explained in the followings.

It should be pointed out that, apart from the shove test, the shear-compression tests were performed on companion sample. The initial shear strength and both the initial and the residual friction coefficient of the companion samples (triplets) were found as 0.13 MPa and 0.46, respectively.

4 Numerical Model

Numerical simulations of the shove test were conducted with the aim of investigating which parameters could affect the sliding behavior experimentally observed. In particular, the evolution of the stress state along the sliding brick was studied with the objective of accurately assess the vertical compressive stress in each test phase. Moreover, the possible effect of dilatancy on the test outcomes was analyzed as well.

4.1 Modeling Strategy

The modeling of masonry structures can be performed according to different approaches, namely macro-modeling or micro-modeling approaches [4], depending on the desired level of accuracy (e.g. modeling masonry as a composite or modeling the constituents). To properly model the sliding failure of a single brick in the shove test, a simplified micro-model was chosen, in which the single components (bricks and mortar) were taken into account. In particular, a simplified strategy was adopted: the mortar joints were modeled using 3-noded zero-thickness interface elements and the brick units were modeled using quadratic 8-noded plane stress elements with expanded geometry, so to maintain the overall dimensions of the wall unchanged.

The numerical simulations were performed with the finite element software DIANA FEA (Release 10.1). A 2D model was considered, given that the experimental test was performed on a single-wythe wall. The nonlinear analyses were carried out by imposing an increasing horizontal load both to the tested and the contrast brick, to reproduce the presence of the horizontal hydraulic jack. Regular Newton-Raphson method and arc-length method were adopted to solve the nonlinear problem.

The nonlinear behavior was lumped at the interface elements where the sliding failure was expected to take place, while the bricks were modelled as continuum elements with linear elastic behavior. To define the normal and shear stiffness of the interface elements, k_n and k_t, the elastic moduli of the bricks and mortar were adopted as proposed in Ref. [5]. The nonlinear behavior at the brick-mortar interface was described with a composite interface model, including a tension cut-off, a Coulomb friction criterion and a compressive cap. Exponential softening for tension and shear failure modes was included, while a hardening/softening behavior was introduced for compression. The complete description of the numerical implementation is not reported here, but the reader can refer to Ref. [6]. A no-tension material behavior was assigned to horizontal and vertical joints, with a constant normal stiffness for compression and a zero stiffness for tension. No connection was considered between the edges of the flat-jacks holes.

With reference to the Coulomb friction model, which describes the shear-sliding behavior observed in the experimental test, the yielding function reads:

$$f(\sigma, \kappa_2) = |\tau| + \sigma \cdot \left[\tan \phi_0 + (\tan \phi_{res} - \tan \phi_0) \cdot \frac{c_0 - c(\kappa_2)}{c_0} \right] - c_0 \cdot \exp\left(-\frac{c_0}{G_f^{II}} \kappa_2 \right). \tag{3}$$

In Eq. (3), where the cohesion and friction softening are included, c_0 is the cohesion of the brick-mortar interface, ϕ_0 and ϕ_{res} are the initial and the residual friction angle, respectively, G_f^{II} is the mode-II fracture energy, and κ_2 is a scalar indicating the amount of softening, assumed equal to the plastic shear displacement.

A non-associated plastic potential g_2 is considered, with a variable dilatancy angle ψ, depending on the normal stress and the plastic shear displacement, according to the proposal of Van Zijl [7]:

$$g_2 = |\tau| + \sigma \cdot \left[\tan \psi_0 1 - \frac{\sigma}{\sigma_u} e^{-\delta v_p} \right] - c_0 \tag{4}$$

where v_p is the plastic shear displacement, ψ_0 is the dilatancy angle at zero confining stress and shear slip, σ_u is the pre-compression level at which the dilatancy goes to zero, and δ is the dilatancy shear-slip degradation coefficient.

4.2   Calibration of the Model

The input parameters used in the numerical model for masonry are reported in Table 2, where distinction is made between parameters obtained directly from tests and calibrated ones. Concerning parameters obtained from tests, the elastic modulus of bricks, together with the masonry compressive strength f_c and the compressive fracture energy G_f^c, were determined through uniaxial compression tests on the single components and on masonry wallets. The mechanical properties describing the Coulomb friction failure criterion were determined by performing triplet tests on companion specimens, according to the Standard EN1052-3 [8]. Concerning calibrated parameters, results of compression tests on masonry wallets were used to evaluate the elastic modulus of the mortar and the Poisson's ratios of bricks and mortar. Tensile strength and mode-I fracture energy were determined as a fraction of the cohesion and mode-II fracture energy, respectively [5]. The parameters defining the dilatancy function (Eq. 4) and the mode-II fracture energy function were calibrated from standard triplet tests results, as described in [9]. Considering that the shear-sliding mechanism observed in triplet tests is the same occurring in the shove test, the same calibrated parameters were used to model the shove test presented in Sect. 2.

4.3   Numerical Results

In the numerical simulations, the same nominal overburden adopted in the experimental test was applied at the top of the wall, and the first four flat-jack pressure steps were

Table 2. Input parameters for masonry: (a) parameters from tests; (b) calibrated parameters.

	Description	Symbol	Units	Value
Parameters from tests	Elastic modulus of brick	E_b	[N/mm²]	10000
	Cohesion	c_0	[N/mm²]	0.13
	Friction angle	ϕ_0	[rad]	0.463
	Residual friction angle	ϕ_{res}	[rad]	0.463
	Compressive strength	f_c	[N/mm²]	6.35
	Compr. fracture energy	G_f^c	[N/mm]	20
	Equiv. plastic shear displ.	κ_p	-	0.005

(a)

	Description	Symbol	Units	Value
Calibrated parameters	Poisson's ratio of brick	v_b	-	0.16
	Elastic modulus of mortar	E_m	[N/mm²]	1088
	Poisson's ratio of mortar	v_m	-	0.20
	Interface normal stiffness	k_n	[N/mm³]	122.1
	Interface shear stiffness	k_t	[N/mm³]	50.7
	Tensile strength	f_t	[N/mm²]	0.09
	Mode-I fracture energy	G_f^I	[N/mm]	0.01
	Dilatancy angle	ψ_0	[rad]	0.374
	Confining normal stress	σ_u	[N/mm²]	0.58
	Exp. degradation coeff.	δ	-	9.63
	Mode-II fracture energy	a	[mm]	0.114
	$(G_f^{II} = a\sigma + b)$	b	[N/mm]	0.011

(b)

considered. The comparison between numerical and experimental results is given in Fig. 3, in terms of shear stress τ *vs* tangential displacement δv, and vertical displacement δu *vs* tangential displacement δv. The dashed line in the first step of the experimental curve, highlights the fact that the post-peak phase could not be correctly controlled. In Fig. 3b, only the first step is considered, given that dilatancy is effective for low values of the plastic tangential displacement.
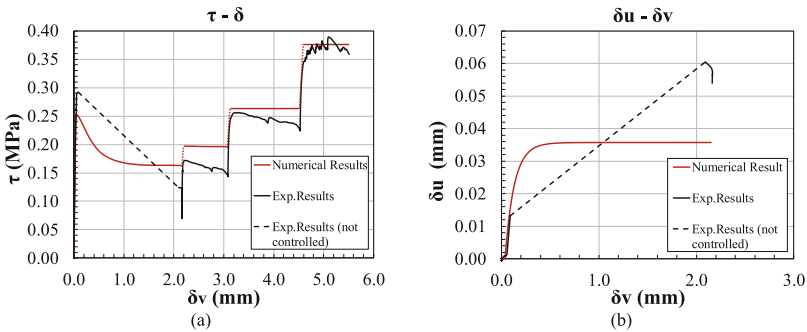
Fig. 3. Numerical results: (a) shear stress *vs* tangential displacement; (b) orthogonal displacement *vs* tangential displacement

It is possible to notice that, in the first step, a lower peak stress and a higher residual stress were obtained in the numerical analysis with respect to the experimental results. A slight difference between the failure criteria observed from triplet tests (used for calibration) and that from shove test results, in correspondence of a low compressive stress, can determine these discrepancies. In the subsequent load steps, instead, a better agreement was found, especially in the third and fourth steps. A very good agreement can be noticed in the first part of the graph of Fig. 3b. However, when the peak load is attained, the experimental orthogonal displacements are much higher than the ones

obtained from the numerical analysis. This can be related to the fact that, during the test, rigid movements of the sliding brick (e.g. rotation) influenced the final value of the orthogonal displacements. Worth mentioning that their absolute value is small and thus sensitive even to limited experimental anomalies.

As already mentioned, the compressive state of stress on the sliding brick is not uniform and it is significantly influenced by the testing procedure. In order to evaluate this variation, a numerical analysis is carried out to calibrate correction factors related to the stress distribution in the different phases of the test. To this purpose, the vertical stress distributions were evaluated for the top and bottom sliding joints during the removal of bricks and the application of the flat-jack pressure. The average compressive stress was calculated and compared with the nominal value applied (as overburden or as flat-jack pressure) in that phase. By doing so, the overburden correction factor and the flat-jack to brick correction factor resulted to be equal to 0.64 and 1.21, respectively. It can be noticed that the flat-jack to brick correction factor is very similar to the one experimentally obtained (1.18). By correcting the nominal pre-compression stress values with these coefficients, as explained in Sect. 3, a reliable calibration of the residual failure criterion can be achieved. In particular, by considering modified pre-compression values, accounting for both the flat-jack and the overburden contributions, a residual cohesive shear strength value very close to zero is obtained. The value of the coefficient of friction, instead, remains unchanged and equal to 0.55.

5   Conclusions

To gain a better insight into the shear-sliding behavior of masonry during the shove test, both experimental test and numerical simulations were adopted in the current research. The experimental tests were performed in the controlled laboratory environment on a replicated calcium silicate brick masonry wall. A well-designed acquisition system allowed the continuous measurements of the applied load and the corresponding deformations. Experimentally, the contribution of the flat-jack pressure to the compressive stress of the sliding brick was investigated. Moreover, the contribution of the overburden load to the compressive stress of the sliding brick was numerically evaluated. In particular, in this work, correction factors for the distributions of the vertical load and for flat-jack pressure, as proposed in Ref. [3], were evaluated for the masonry typology investigated. The actual vertical stress state on the sliding brick was evaluated as the sum of the flat-jack contribution (given by the flat-jack pressure multiplied by the flat-jack to brick correction factor) and the overburden contribution (given by the overburden pressure multiplied by the overburden correction factor). By considering the actual vertical stress, a consistent residual failure criterion was obtained. Given that dilatancy did not significantly influence the experimental results in terms of capacity, the evaluation of these two contributions only was sufficient for the correct estimation of the compressive stress state on the brick. The numerical model is capable of reproducing the shear-sliding failure mode experimentally observed in the shove test and of estimating the actual compressive state of stress, which helped in the calibration of the residual failure criterion. The simplified micro-modeling strategy with the combined interface model confirmed to be adequate to

study the shear-sliding phenomenon and it is a useful tool for the interpretation of the results.

References

1. ASTM C1531 (2016) Standard Test Methods for In Situ Measurement of Masonry Mortar Joint Shear Strength Index. American Society for Testing and Materials (ASTM) International
2. Noland JL, Kingsley GR, Atkinson RH (1988) Utilization of non-destructive techniques into the evaluation of masonry. In: Proceedings of the 8th international brick/block masonry conference, Dublin, October 1988
3. Rossi A, Graziotti F, Magenes G (2015) A proposal for the interpretation of the in-situ shear strength index test for brick masonry. In: Proceedings of the ANIDIS conference, L'Aquila (Italy)
4. Lourenço PB, Rots JG, Blaauwendraad J (1995) Two approaches for the analysis of masonry structures: micro and macro-modeling. Heron 40(4):313–340
5. Rots JG (1997) Structural masonry – an experimental/numerical basis for practical design rules. Balkema, Rotterdam
6. Lourenço PB (1996) Computational strategies for masonry structures. Ph.D. thesis, Delft University of Technology
7. Van Zijl G (2004) Modeling masonry shear-compression: role of dilatancy highlighted. J Eng Mech 130(11):1289–1296
8. EN 1052-3 (2002) Method of test for masonry – part 3: determination of initial shear strength. European Standards (EN)
9. Ferretti F, Esposito R, Rots JG, Mazzotti C (2018) Shear-sliding behavior of masonry: numerical micro-modeling of triplet tests. In: Proceedings of the EURO-C conference, Austria